Effect of a pH Change on the Conformational Stability of the Modified Nucleotide Queuosine Monophosphate

Dmytro Kosenkov,[†] Yana A. Kholod,[†] Leonid Gorb,[‡] Oleg V. Shishkin,[§] Gulnara M. Kuramshina,[||] Galina I. Dovbeshko,[⊥] and Jerzy Leszczynski*[,†]

Interdisciplinary Center for Nanotoxicity, Department of Chemistry, Jackson State University, Jackson, Mississippi 39217, Department of Molecular Biophysics, Institute of Molecular Biology and Genetics, National Academy of Sciences of Ukraine, 150 Zabolotnoho, Kiev 03143, Ukraine, STC "Institute for Single Crystals", National Academy of Sciences of Ukraine, 60 Lenina Avenue, Kharkiv 61001, Ukraine, Department of Chemistry, Moscow State University, 119991 Moscow, Russia, and Department of Physics of Biological Systems, Institute of Physics, National Academy of Sciences of Ukraine, 46 Prospekt Nauki, Kiev 02038, Ukraine

Received: April 30, 2009; Revised Manuscript Received: June 25, 2009

The naturally occurring modified nucleotide queuosine 5′-monophosphate (QMP) related to biochemical regulatory pathways in the cell was investigated using quantum chemical approaches. The relative stability of biologically relevant conformations of QMP in solvent under a pH change was predicted at the BVP86/TZVP and MP2/TZVP levels of theory. Hydrogen bonding in QMP was studied using Bader's approach. The acidity constants of QMP were estimated using the COSMO-RS theory. It has been found that the neutral and anionic forms of QMP are the most stable in the physiological pH range. These forms correspond to the *anti*/*north* conformation and exist as zwitterionic tautomers having a negatively charged phosphate group (−1 for neutral and −2 for anionic) and a positively charged secondary amine group in the side chain. It was also found that QMP possesses the *syn* conformation in the cationic state at pH < 5.0 and undergoes *syn* to *anti* conformation transition when the pH increases, remaining in the *anti* conformation at the higher pH values. The marker IR bands specific for the anionic and neutral QMP forms in the 2300−2700 cm^{-1} region were assigned to H-bonded NH groups of the QMP side chain. The bands between 800 and 1300 cm^{-1} of the "fingerprint" (400−1500 cm^{-1}) region were assigned to the vibrations of the ribose ring, the phosphate group and the side chain of QMP. The predicted IR spectra can be useful for the assignment of vibration bands in the experiential spectra of QMP or identification of the QMP forms. The revealed peculiarities of the QMP conformation sensitivity to a pH change as well as additional formed H-bonds could be responsible for specific nucleotide interactions with enzymes.

Introduction

The structure of queuosine (Q) has been experimentally studied using gas chromatography, mass spectroscopy,[1] and X-ray diffraction[2] methods. It has been shown that the structure of queuosine corresponds to 7-[[(4,5-*cis*-dihydroxy-1-cyclopenten-3-yl)amino]methyl]-7-deazaguanosine. Nucleoside Q substitutes guanosine in the 34 position of the anticodon stem−loop region of the tRNA. It has been revealed that Q is present in almost all life forms from *Escherichia coli* to *Homo sapiens*.[3] The correlation between the amount of queuosine and dysfunction of cell growth and division as well as the response to an external impact has been observed.[4−8] Human tumor biopsies demonstrate a difference in the quantity of queuosine-modified tRNA for tumors with different metastatic potentials.[4−8] It was also found[9,10] that cancer transformation of the cell leads to changes in the RNA structure and results in its disordering including damage in the primary, secondary, and tertiary structure of RNA and redistribution of the H-bond network which is connected with the modification of the nucleosides. Recent progress in enzymology[11−14] suggests that incorporation of queuosine into tRNA, where it is present in the forms of queuosine 5′-monophosphate (QMP), proceeds via a complex biochemical pathway involving several enzymes. Since QMP and its precursors participate in complex biochemical enzymatic transformations, one may expect that queuosine conformations play an important role in nucleoside−enzyme interactions.

The computational studies of QMP using semiempirical (PCILO, PM3), ab initio (HF, DFT),[15] and molecular mechanics[16] methods have been carried out. The molecular mechanics study[16] of the QMP effect on the tRNA structure and function has revealed increasing anticodon loop rigidity. However, QMP does not alter Watson−Crick pairing in tRNA.[16] The possibility of formation of additional H-bonds in QMP in comparison to canonic guanosine 5′-monophosphate has been suggested.[15] In addition, it has been hypothesized[15] that protonation of QMP could affect the conformation of the molecule and change the pattern of intra- and intermolecular hydrogen bonding.[15] The effect of protonation on canonic nucleotide conformations has also been observed in our previous works.[17−20]

Since QMP has both proton acceptor (phosphate, PO_4^{3-}) and proton donor (secondary amino, NH_2^+) groups, the predominant

* To whom correspondence should be addressed. Phone: (601) 979-3723. Fax: (601) 979-7823. E-mail: jerzy@icnanotox.org.
[†] Jackson State University.
[‡] Institute of Molecular Biology and Genetics, National Academy of Sciences of Ukraine.
[§] STC "Institute for Single Crystals", National Academy of Sciences of Ukraine.
[||] Moscow State University.
[⊥] Institute of Physics, National Academy of Sciences of Ukraine.

10.1021/jp903993s CCC: $40.75
Published on Web 07/24/2009

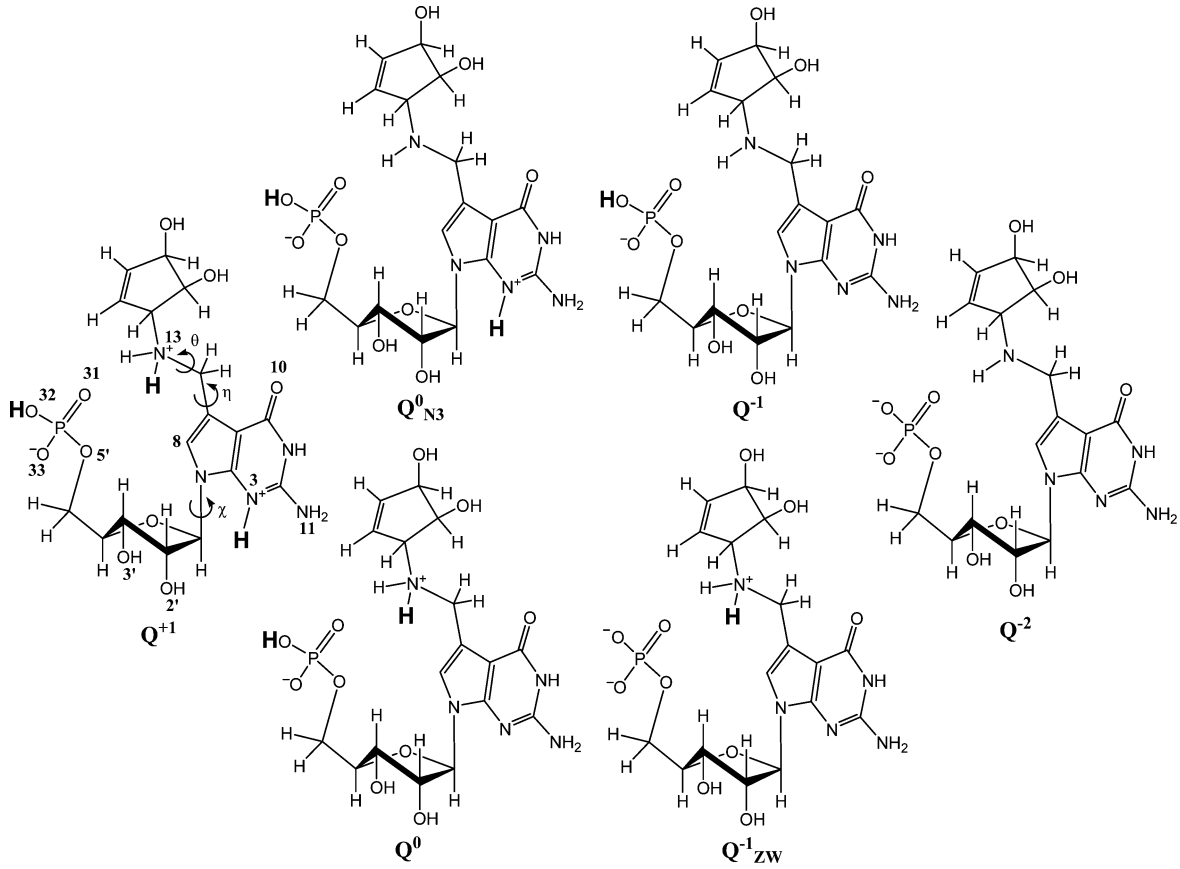

Figure 1. Considered protonation forms of QMP. Protons removed under deprotonation are shown in bold. The dihedral angle χ characterizes the mutual orientation of the purine and ribose rings. The orientation of the (cyclopentenylamino)methyl side chain is described by dihedral angles η and θ. Only the *anti*/*north* conformation is shown.

molecular forms of QMP which are present in aqueous solution will depend on the pH of the solution. This makes QMP to some extent similar to amino acids that incorporate both proton donor and acceptor groups and have pronounced pH titration behavior. To investigate the effect of the pH on the molecular characteristics, acid-ionization constants (pK_a) should be evaluated. The calculation of pK_a of the proton donor and acceptor groups is quite challenging,[21] but the knowledge of these properties is essential[22] for the understanding of the structure and functionality of the amino acid and protein molecules. In the present study, to investigate the effect of the pH on QMP, the values of pK_a have been evaluated. Since the thermodynamic properties and functionality of proteins and nucleic acids[23] depend on solvation and pK_a evaluation requires estimation of solvation energies, solvent effects should be included in the calculations. Due to their computational efficiency and accuracy the continuum solvent models are commonly used in such predictions. In the current study, to account for the solvent effects, the extension of the conductor-like screening model (COSMO)[24,25] (which includes the polarity distribution calculated by ab initio methods and relies on a large number of experimental data) called the COSMO-RS (COSMO for real solvent) technique[26−28] has been used.

The goal of the present study is to investigate biologically relevant conformations and reveal crucial H-bonds of QMP in water solution and to estimate the relative stability of the conformers under a pH change within the COSMO-RS model. The most stable conformers under physiological pH will be additionally characterized using simulated IR spectra.

Methods of Calculation

The initial geometries of the nucleotide were taken from X-ray data.[2] The conformations of QMP that were not observed in X-ray studies were designed on the basis of our previous studies on canonic nucleotides.[17,18] On the basis of the results of X-ray data[2] and molecular dynamics simulations on nucleosides in solution,[29] typical biologically relevant conformations (according to Saenger's notation)[30] with *syn* and *anti* orientations of the purine ring with respect to the ribose five-membered ring as well as conformations with a *south* (C2′-*endo*) and *north* (C3′-*endo*) sugar pucker (Figure 2) were investigated.

To study the pK_a of different protonation states, cationic (Q^+), neutral (Q^0, Q^0_{N3}), anionic (Q^-, Q^-_{ZW}), and dianionic (Q^{2-}) forms are considered (Figures 1 and 2). These forms differ in the number of protons (shown in bold in Figure 1) on the phosphate group and in the side chain of QMP.

Density functional theory calculations were performed with the Gaussian03[31] program. The optimized geometries of the compounds studied were calculated at the BVP86/TZVP[32,33] level of theory using Ahlrichs's triple-ζ basis set.[34,35] Single-point energies were also calculated at the MP2/TZVP level using a reference BVP86/TZVP geometry.

The influence of the solvent environment was considered within the COSMO approach.[24,25] Acid-ionization constants for QMP at 298 K were calculated using the COSMO-RS technique,[26,27] which is implemented in the COSMOtherm program package.[28] COSMO-RS treats a polarization charge density calculated with the COSMO option of the Gaussian03[31] program. The QMP energy in solvent was estimated as a sum

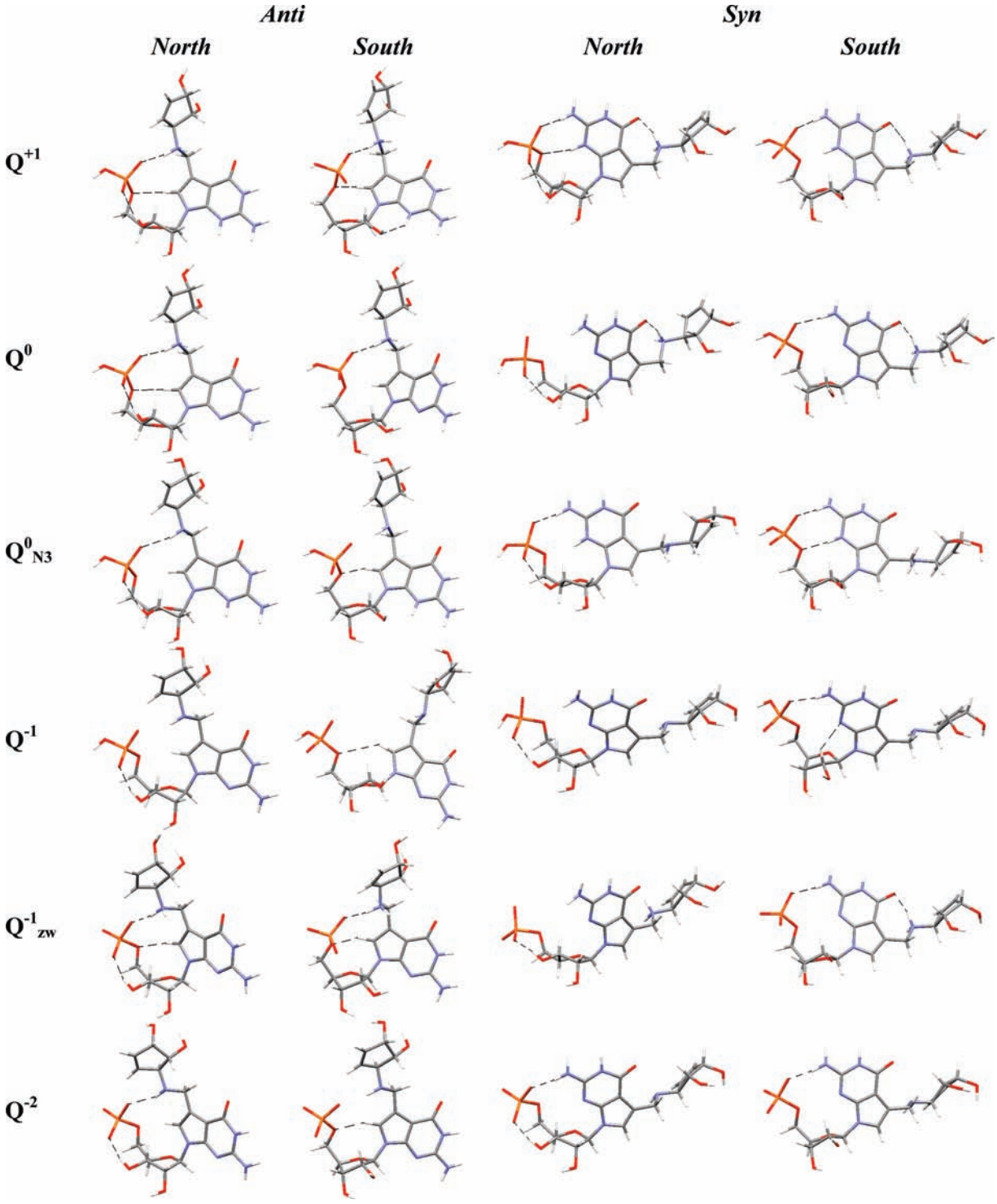

Figure 2. Considered conformations of the QMP forms. Dashed lines represent H-bonds.

of either the BVP86/TZVP or the MP2/TZVP electronic energy plus the COSMO-estimated free energy of solvation.

The frequencies of the normal vibrations were calculated at the same level of theory within harmonic approximation. The solvent effects during spectral calculation were accounted for using the COSMO solvent model.

The software package SPECTRUM[36] was used for transformation of quantum mechanical force constants in Cartesian coordinates to the canonical matrix in redundant internal coordinates.[37] Normal coordinate analysis for all investigated systems was carried out using SPECTRUM, and the potential energy distribution was calculated in accordance with the approach.[38,39]

A topological analysis of the electron density distribution was carried out within Bader's "atoms in molecules" (AIM) approach[40] in the AIM2000 program[41] using the wave function obtained at the BVP86/TZVP level of theory. The existence of intramolecular hydrogen bonds was established on the basis of the presence of the specific type of the critical point of electron density between two covalently nonbonded atoms. This point is called the bond critical point (BCP) and belongs to a saddle-type critical point (minimum of the electron density along the

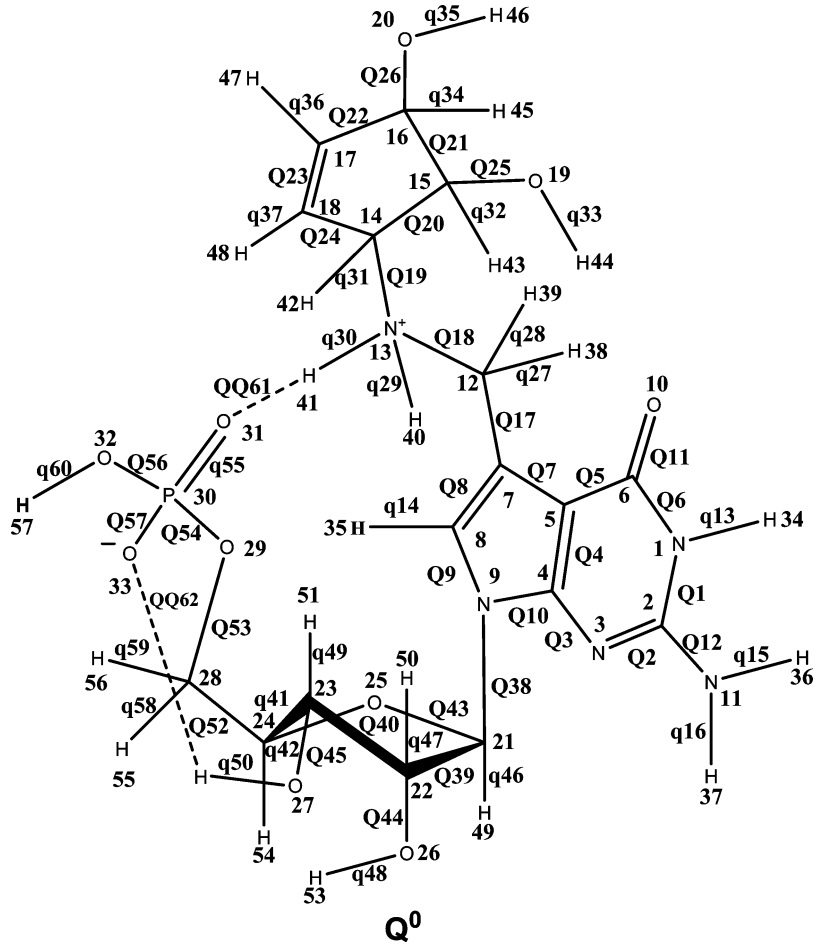

Figure 3. Atom and bond designations of Q^0 used for evaluations of the potential energy distribution presented in Table 5.

line which connects two atoms and maximum in perpendicular directions). For hydrogen bonds the value of the electron density (ρ) in a BCP should be in the range 1.5×10^{-2} to 3.5×10^{-2} e/au^3,[42,44] and the Laplacian of the electron density ($\nabla^2\rho$) in a BCP should be in the range 4.4×10^{-2} to 13.9×10^{-2} e/au^5.[42−44] Following previous works,[42,45,46] the distance between the RCP (ring critical point) and BCP was considered to be $L_{RCP} > 1.5$ au for strong H-bonds and $L_{RCP} > 1.1$ au for weak H-bonds of the C−H···O or C−H···N type. The ellipticity ($\varepsilon = \lambda_1/\lambda_2 - 1$) provides a measure of the extent to which the charge is preferentially accumulated in the given plane.[45] According to previous studies,[42,46] if the hydrogen bond exists, the ellipticity should be $\varepsilon < 0.09$ for strong and $\varepsilon < 0.22$ for weak H-bonds.[42,47] Following Espinosa et al.,[48] using the relation between the local potential energy (V) and the H-bond energy (E_{HB}) in BCP, $E_{HB} = -V/2$, the energy of a H-bond can be written as follows:

$$E_{HB} = \frac{1}{2}\nabla^2\rho\left(\frac{\hbar^2}{4m} - \frac{1}{3}\right) + \frac{3}{10}(3\pi^2)^{2/3}\rho^{5/3} \qquad (1)$$

where ρ is the electron density and $\nabla^2\rho$ is the Laplacian of the electron density in the BCP. It was demonstrated that energies of intermolecular interactions calculated in this way agree with other quantum-chemical data.[42,47,49]

Results and Discussion

Geometry of the Nucleotide. Optimized structures of QMP species are presented in Figure 2. Selected geometry parameters of the molecules are collected in Table 1. The mutual position of the QMP subunits was characterized following by Saenger.[30] The dihedral angle χ characterizes the mutual orientation of the purine and ribose rings. The *anti* conformations of the nucleotide correspond to a χ range of −178.2° (Q^0, *anti*/*south*) to −113.7° (Q^{2-}, *anti*/*south*), while *syn* conformations have $\chi = 38.5°$ (Q^+, *syn*/*north*) to 0.86.8° (Q^-_{ZW}, *syn*/*north*). The ribose ring conformation is described by the pseudorotation phase angle (P) and maximum out-of-plane pucker (ν_{max}). The *north* conformers correspond to a P range of 3.7° (Q^-_{ZW}, *anti*/*north*) to 0.46.7° (Q^-, *syn*/*north*) and to a C3′-*endo* sugar pucker. The *south* conformers have values of $P = 152.3°$ (Q^0_{N3}, *syn*/*south*) to 0.189.1° (Q^+, *anti*/*south*) and possess a C2′-*endo* conformation. The maximal sugar pucker $\nu_{max} = 41.0°$ (Q^+, *anti*/*north*) to 44.8° (Q^-_{ZW}, *syn*/*north*) is observed in *north* conformations where the O(3′)−H···O(33) hydrogen bond is present. The orientation of the (cyclopentenylamino)methyl side chain is described by dihedral angles η and θ (Figure 1). The angle $\theta = 172.9°$ (Q^-_{ZW}, *syn*/*south*) to 0.189° (Q^{2-}, *anti*/*south*) has minor changes, while the angle $\eta = -142.6°$ (Q^{2-}, *anti*/*south*) to −47.8° (Q^0, *syn*/*north*) changes significantly under conformational transitions in other parts of the molecule. The angle η has a lower value, −80.9° (Q^-, *anti*/*south*) to −142.6° (Q^{2-}, *anti*/*south*), in *anti* conformations of QMP, which can be rationalized in terms of hydrogen bonding.

Hydrogen Bonding. The parameters of the AIM analysis that characterize hydrogen bonding in different QMP species are collected in Table 2. The analysis of these data revealed that the orientation of the modified fragment is stabilized by a

TABLE 1: Selected Geometrical Parameters of QMP Conformers[a]

		χ, deg	P, deg	ν_{max}, deg	ribose conformation[b]	η, deg	θ, deg
Q^+	*anti/north*	−165.5	6.0	41.0	$^3T_2$	−100.2	177.7
	anti/south	−174.8	189.1	34.3	$_3T^2$	−81.3	187.8
	syn/north	38.5	36.2	41.1	$_4T^3$	−56.6	177.7
	syn/south	55.4	153.1	35.6	$^2T_1$	−52.1	175.5
Q^0	*anti/north*	−166.9	4.7	41.5	$^3T_2$	−99.4	176.9
	anti/south	−178.2	188.9	33.0	$_3T^2$	−80.1	180.7
	syn/north	67.9	43.4	42.2	$_4T^3$	−47.8	173.3
	syn/south	73.3	154.1	35.7	$^2T_1$	−48.2	172.3
Q^0_{N3}	*anti/north*	−162.4	8.6	40.9	$^3T_2$	−101.5	181.7
	anti/south	−164.9	185.3	32.3	$_3T^2$	−85.8	188.8
	syn/north	42.3	39.0	41.1	$_4T^3$	−78.6	182.5
	syn/south	55.2	152.3	35.6	$^2T_1$	−79.6	181.8
Q^-	*anti /north*	−151.2	9.1	40.4	$^3T_2$	−118.6	185.7
	anti/south	−115.3	158.6	37.1	$^2T_1$	−80.9	184.5
	syn/north	73.3	46.7	43.6	$_4T^3$	−85.2	184.8
	syn/south	74.4	152.8	36.6	$^2T_1$	−81.4	185.9
Q^-_{ZW}	*anti/north*	−160.6	3.7	41.2	$^3T_2$	−106	174.7
	anti/south	−152.9	182.4	33.1	$_3T^2$	−102	175.4
	syn/north	86.8	34.8	44.8	$^3T_4$	−86.2	181.2
	syn/south	73.3	157.8	37.7	$^2T_1$	−48.8	172.9
Q^{2-}	*anti/north*	−148.5	8.9	40.8	$^3T_2$	−121	186.1
	anti/south	−113.7	185.1	30.6	$_3T^2$	−142.6	189.0
	syn/north	64.3	35.6	39.0	$^3T_4$	−82.7	185.5
	syn/south	74.3	156.7	36.8	$^2T_1$	−83.7	186.1

[a] Angles χ, η, and θ are defined in Figure 1. Parameters P and ν_{max} describe the ribose ring. [b] Ribose conformations are defined in accordance with ref 27.

H-bond of the N−H···O type. In *syn* conformations of Q^+, Q^0, and Q^-_{ZW} species the side chain orientation is stabilized by the N(13)−H···O(10) H-bond between the nitrogen of the side chain and the oxygen of 7-deazaguanine. In *anti* conformations except that of Q^- the N(13)−H···O(31) bond between the side chain and the phosphate group stabilizes the orientation of the side chain. The switching between N(13)−H···O(10) and N(13)−H···O(31) H-bonds under *syn* to *anti* transition explains the dependence of the angle η (Table 1) on the nucleotide conformation. The hydrogen bond C(8)−H···O(5′) between 7-deazaguanine and the oxygen of the phosphate group also contributes to stabilization of the *anti* conformation. All *syn/south* and *syn/north* conformations of Q^+, Q^0_{N3}, and Q^{2-} are stabilized by the N(11)−H···O(31) hydrogen bond.

Similarly to canonic nucleotides,[17] the *north* conformation of the ribose ring is stabilized by a strong O(3′)−H···O(33) hydrogen bond between the ribose moiety and the phosphate group. This makes the *north* conformations energetically favorable over the *south* ones (Table 3).

Many of the considered H-bonds of N−H···O, O−H···O, and C−H···O types are formed by the negatively charged phosphate group and positively charged nucleobase or neutral ribose moieties. Therefore, the effect of charge assistance on the H-bonding[42] should be considered.

A common trend for all H-bonds found in the system is their strengthening with an increase of both the negative charge of the phosphate group and the positive charge of the N(13) atom of the secondary amine group. Another trend is obvious: the strongest H-bonds are formed between groups with opposite charges. However, each type of the considered H-bonds has certain peculiarities. Namely, the N(13)−H···O(31) bond is the strongest (18.63 kcal/mol) in the Q^-_{ZW} form, and it is disrupted under deprotonation of the N(13)H group. The H-bond N(11)−H···O(31) depends on protonation of the N(3) site. The protonation of the N(3) site results in the more acidic $N(11)H_2$ amino group and a stronger N(11)−H···O(31) bond. The strongest N(11)−H···O(31) bond (17.43 kcal/mol) is formed in the Q^+ state. The C(8)−H···O(5′) hydrogen bond mainly depends on the charge of the phosphate group and is the strongest (5.25 kcal/mol) in the dianionic Q^- form. Finally, the H-bond O(3′)−H···O(P1) follows the general trend and has its maximum value in the Q^-_{ZW} form.

Relative Energies of the Conformers. The relative energies of the conformers in solvent were estimated using both the BVP86/TZVP and MP2/TZVP levels. The results are collected in Table 3. Since electronic energies calculated using second-order Møller−Plesset perturbation theory are generally more accurate than energies calculated using DFT methods, MP2/TZVP energies will be considered below. The results suggest that the relative stability of QMP conformers depends on the protonation states of the nucleotide. QMP in the cationic form (Q^+) possesses the *syn* conformation, which is ca. 5 kcal/mol more stable than the *anti* one. According to the MP2/TZVP estimation, the *syn/north* conformation of Q^+ is 2.45 kcal/mol more stable than the *syn/south* conformation. The neutral form of QMP with an $-N(13)H_2^+-$ group (Q^0) is ca. 5−20 kcal/mol more stable than the N(3)-protonated Q^0_{N3} form. In the neutral form Q^0 the *anti/north* conformation is 6.45 kcal/mol more stable than the other conformations. Among the anionic forms (Q^-, Q^-_{ZW}) the *anti/north* conformation of the Q^-_{ZW} form is the most stable. The same *anti/north* conformation is preferable for the dianionic form (Q^{2-}). It was revealed that *anti/north* conformers are the most stable for all species with the exception of the Q^+ form. Similar results were obtained for canonic nucleotides in the gas phase,[17] where the *syn* conformation is more stable in the neutral form while the *anti* conformation is more stable in the anionic form. This trend can be explained by the effect of negatively charged phosphates and by the solvent effects. As in our previous study,[18] where the effect of solvent was accounted for through addition of water molecules explicitly, in the present study an application of the COSMO model of solvent also shifts the equilibrium toward stabilization of the *anti* conformers. The *north* conformation of the ribose moiety is always preferred over the *south* one.

TABLE 2: Selected Parameters for Hydrogen Bonds: Distances (D−H···A and H···A), Angle (D−H···A), Electron Density (ρ), Laplacian of the Electron Density ($\nabla^2\rho$), Ellipticity (ε), at Bond Critical Points, Distance to the Ring Critical Point (L_{RCP}), and Estimated Energies of Intramolecular Hydrogen Bonds (E_{HB}) in QMP Conformers

		D−H···A	H···A, Å	D−H···A, deg	100ρ, e/au^3	$100\nabla^2\rho$, e/au^5	L_{RCP}, au	ε	E_{HB}, kcal/mol
Q^+	*anti/ north*	O(3′)−H···O(33)	155.9	1.827	2.44	10.11	2.619	0.07	6.34
		C(8)−H···O(5′)	151.7	2.183	1.78	6.70	1.599	0.02	3.94
		N(13)−H···O(31)	167.3	1.680	4.94	11.60	2.784	0.04	15.02
	anti/south	C(8)−H···O(5′)	114.7	2.377	1.60	5.08	1.397	0.18	3.16
		N(13)−H···O(31)	171.2	1.705	4.53	10.61	3.001	0.09	13.15
		N(3)−H···O(2′)	141.2	2.045	1.43	5.38	1.530	0.14	2.92
	syn/north	O(3′)−H···O(33)	156.7	1.833	2.88	10.19	2.601	0.07	7.54
		N(11)−H···O(31)	168.9	1.667	4.84	13.00	2.483	0.09	14.98
		N(3)−H···O(5′)	164.8	2.019	2.17	7.06	1.470	0.01	4.89
		N(13)−H···O(10)	155.2	1.873	2.46	8.71	1.853	0.09	6.03
	syn/south	N(11)−H···O(31)	171.9	1.635	5.39	13.68	2.397	0.05	17.43
		N(13)−H···O(10)	158.0	1.838	2.67	8.29	1.856	0.09	6.46
Q^0	*anti/north*	O(3′)−H···O(33)	155.9	1.827	2.62	10.17	2.622	0.04	6.82
		C(8)−H···O(5′)	112.5	2.183	1.77	6.61	1.583	0.02	3.89
		N(13)−H···O(31)	167.3	1.682	5.02	11.19	2.823	0.05	15.23
	anti/south	N(13)−H···O(31)	173.0	1.635	4.79	12.33	2.446	0.13	14.61
	syn/north	O(3′)−H···O(33)	164.7	1.699	4.67	12.61	2.396	0.07	14.21
		N(13)−H···O(10)	163.3	1.743	3.68	12.66	1.495	0.06	10.65
	syn/south	N(11)−H···O(31)	176.4	1.839	2.25	6.97	3.022	0.15	5.05
		N(13)−H···O(10)	164.2	1.720	3.51	10.01	1.424	0.21	9.40
Q^0_{N3}	*anti/north*	O(3′)−H···O(33)	158.7	1.781	3.80	10.95	2.870	0.04	10.60
		N(13)−H···O(31)	165.6	2.115	1.72	6.40	1.958	0.05	3.74
	anti/south	C(8)−H···O(5′)	123.4	3.554	1.61	5.38	1.383	0.15	3.26
	syn/north	O(3′)−H···O(33)	156.6	2.786	3.33	10.87	2.504	0.05	9.05
		N(11)−H···O(31)	170.2	2.733	3.54	10.29	2.531	0.06	9.57
	syn/south	N(11)−H···O(31)	173.6	1.652	4.24	9.80	2.351	0.06	11.85
		N(3)−H···O(5′)	174.2	1.881	2.42	8.06	1.865	0.03	5.76
Q^-	*anti/north*	O(3′)−H···O(33)	158.7	1.769	3.87	11.16	2.804	0.04	10.90
	anti/south	C(8)−H···O(5′)[a]	141.2	2.983	0.41	1.24	0.885	0.22	0.51
	syn/north	O(3′)−H···O(33)	166.2	1.693	3.89	8.32	2.401	0.06	10.22
	syn/south	C(2′)−H···N(3)	127.0	2.300	1.62	5.29	1.360	0.06	3.25
		N(11)−H···O(31)	174.1	1.870	2.91	9.90	2.704	0.06	7.55
Q^-_{ZW}	*anti/north*	O(3′)−H···O(33)	162.1	1.655	5.09	10.35	2.771	0.13	15.30
		C(8)−H···O(5′)	161.5	2.069	1.64	7.20	1.493	0.20	3.79
		N(13)−H···O(31)	167.0	1.553	5.72	12.75	2.730	0.13	18.63
	anti/south	C(8)−H···O(5′)	150.6	2.024	2.01	7.73	1.925	0.12	4.70
		N(13)−H···O(31)	171.4	1.544	6.33	16.22	2.732	0.02	22.36
	syn/north	O(3′)−H···O(P1)	168.7	1.587	6.17	13.48	2.376	0.08	20.88
	syn/south	N(11)−H···O(31)	174.2	1.691	4.89	12.16	2.640	0.04	14.96
		N(13)−H···O(10)	164.5	1.721	3.22	8.48	1.431	0.20	8.09
Q^{2-}	*anti/north*	O(3′)−H···O(33)	166.2	1.582	3.83	13.68	3.090	0.04	11.42
		N(13)−H···O(31)	160.2	2.170	1.55	5.72	1.747	0.07	3.23
	anti/south	C(8)−H···O(5′)	144.3	2.157	2.49	5.45	2.203	0.19	5.25
	syn/north	N(11)−H···O(31)	172.0	1.733	3.46	8.56	2.972	0.10	8.86
		O(3′)−H···O(33)	168.8	1.568	5.34	9.27	3.328	0.21	16.07
	syn/south	N(11)−H···O(31)	172.6	1.731	3.38	7.96	2.844	0.14	8.45

[a] According to the considered AIM criteria, this interaction in the Q^- *anti/south* conformation is not an actual H-bond.

TABLE 3: Relative Energies (kcal/mol) of QMP Forms in Solvent Calculated at the MP2/TZVP and BVP86/TZVP (Given in Parentheses) Levels Using the COSMO-RS Model

		anti		*syn*	
total charge	molecule	*north*	*south*	*north*	*south*
+1	Q^+	5.72 (8.45)	11.83 (13.68)	0.00 (0.00)	2.45 (1.21)
0	Q^0	0.00 (0.00)	6.45 (5.22)	7.42 (1.67)	8.16 (2.45)
	Q^0_{N3}	21.69 (18.54)	28.43 (24.40)	12.78 (8.31)	15.57 (9.32)
−1	Q^-	1.93 (3.50)	11.16 (8.26)	6.99 (4.42)	9.27 (6.78)
	Q^-_{ZW}	0.00 (0.00)	10.85 (9.81)	19.70 (13.59)	15.58 (10.21)
−2	Q^{2-}	0.00 (2.32)	8.78 (9.38)	0.74 (0.00)	10.71 (9.81)

Stabilization of the *north* conformation is due to the H-bond between the O(3′)−H group of the ribose ring and the phosphate group. One should also note that the value of the MP2/TZVP energy in solvent difference (at 298 K assuming a Boltzmann distribution) between the *syn/north* and *anti/south* conformers of the dianionic Q^{2-} form, which is equal to ∼0.74 kcal/mol, corresponds to 71% *anti/north* form and 29% *syn/north* form.

Protonation/Deprotonation Effects. Since QMP in aqueous solution may lose or gain protons, the exact probability of QMP protonation (or deprotonation) depends on the pK_a values of the particular proton-donating (proton-accepting) groups of the molecule. One can see that half of the proton-donating (proton-accepting) groups will lose (gain) protons if they are in a solution with pH = pK_a. The higher (lower) the pH value, the more likely

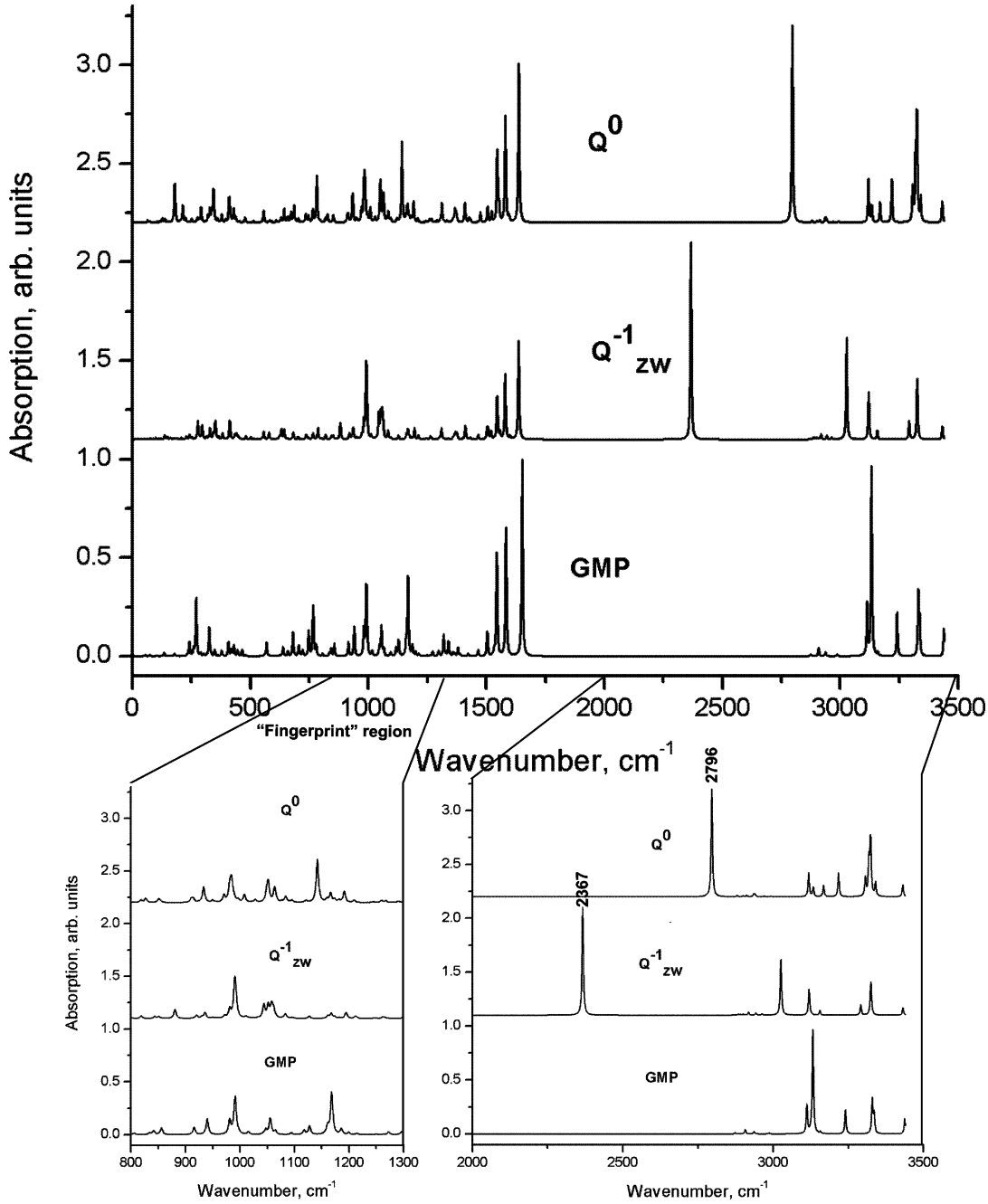

Figure 4. Visualization of the IR spectra of the neutral (Q^0) and anionic (Q^-_{ZW}) forms of QMP in the *north*/*anti* conformation calculated at the BVP86/TZVP level. The spectra are compared with the theoretical spectrum of canonic GMP calculated at the same level of theory. Lorentzian broadening with a half-bandwidth of 5 cm^{-1} is assumed.

QMP will lose (gain) a proton. Since hydrogen bonding and atomic partial charges are perturbed under QMP protonation or deprotonation, the relative stability of QMP conformers depends on the protonation state of the molecule. Therefore, the investigation of the pK_a values of QMP could predict the most stable conformations at different pH values.

The values of pK_a for the most stable conformations (*anti*/*north* and *syn*/*north*) for the corresponding protonation states are presented in Table 4. Analyzing the pK_a values (Table 4) and relative energies of the conformers in solvent (Table 3), one can trace a sequence of QMP transformations under pH change.

The accuracy of our pK_a predictions was estimated using experimental data[50] for N-protonated 2,6-di-*tert*-butylpyridine (4.95) and 2,6-dimethylpyridine (6.75) to compare with $N(3)^+H$

TABLE 4: pK_a Values of the Most Stable (*anti*/*north*, *syn*/*north*) QMP Conformers for the Corresponding Protonation Forms Calculated Using the COSMO-RS Approach

	H[a]	*anti*/*north*	*syn*/*north*
$Q^+ \leftrightarrow Q^0_{N3}$	N(13)	11.3	11.2
$Q^+ \leftrightarrow Q^0$	N(3)	7.0	5.0
$Q^0_{N3} \leftrightarrow Q^-$	N(3)	6.8	5.0
$Q^0 \leftrightarrow Q^-_{ZW}$	O(32)	6.1	6.7
$Q^0 \leftrightarrow Q^-$	N(13)	11.1	11.2
$Q^- \leftrightarrow Q^{2-}$	O(32)	6.3	6.4
$Q^-_{ZW} \leftrightarrow Q^{2-}$	N(13)	11.2	10.9

[a] Atom to which the removed proton had been attached (atom numbering according to Figure 1).

TABLE 5: Frequencies (ω, cm^{-1}), Relative Intensities (I, %), and Potential Energy Distribution (PED, %) of Selected IR Modes of the Neutral (Q^0) and Anionic (Q^-_{ZW}) Forms of QMP in the *north*/*anti* Conformation Compared with Canonic GMP[a]

Q_0			$Q^{-1}{}_{ZW}$			GMP*			
ω	I	PED[b]	ω	I	PED[b]	ω	I	PED[b]	assignment[c]
3431	11	57(q16) 3(q15)	3432	7	57(q16) 43(q15)	3438	14	55(q16) 45(q15)	G: NH_2 str-asym
3341	12	100(q33)	3326	14	84(q33)				P: OH str
3325	20	55(q15) 42(q16)	3326	9	47(q15) 36(q16)	3330	32	55(q15) 45(q16)	G: NH2 str-sym
3324	38	71(q50) 22(q48)	3026	52	95(q50)	3132	96	96(q50)	R: OH str (HB)[d]
3318	31	77(q48) 22(q50)	3324	10	99(q48)	3336	18	100(q48)	R: OH str
3307	17	100(q35)	3292	10	100(q35)				P: OH str
3218	22	100(q60)				3241	22	100(q60)	Pho: OH str
3168	10	99(q14)	3122	4	86(q14) 13(q13)	3158	2	99(q14)	G: CH str
3134	9	99(q29)	3156	4	99(q29)				Y: NH str
3119	22	99(q13)	3120	22	86(q13) 13(q14)	3113	26	100(q13)	G: NH str
2796	100	100(q30)	2367	100	100(q30)				Y: NH str (HB)[d]
					Bands in the "Fingerprint" Region				
1192	11	19(A-9−14) 7(A-8−14)	1195	6	15(A-9−14) 6(A-8−14)	1294	0.4	17(Q7) 14(A-8−14)	G: CH ip bend (5)
1167	9	8(A-25−33) 8(A-20−31)	1168	5	11(A-26−35) 7(A-22−34) 7(A-25−33)				P: OH ip bend, CH bend
1160	3	30(A-44−48)27(A-39−47)	1162	2	27(A-44−48) 26(A-39−47)	1161	7	29(A-39−47) 28(A-44−48)	R: OH ip bend, CH bend
1142	41	46(Q57) 34(Q55)	991	33	34(Q55) 31(Q57) 9(Q19)	1169	40	65(Q55) 22(Q57)	Pho: PO_2 str-asym
1084	5	20(Q6)	1084	4	15(Q6) 7(Q20)	1128	8	34(Q6) 9(Q2) 8(Q7)	G: C−N str (6)
1064	13	66(Q25)	1062	8	65(Q25)				P: C−O str
1052	18	48(Q44) 9(Q40)	1058	12	41(Q56) 23(Q44)7(Q57)	1048	4	38(Q44)	R: C−O(H)str
1050	8	17(Q42) 15(Q52) 14(Q53) 9(A-52−59)	1044	13	19(Q53) 18(Q56) 8(Q52) 7(Q42)	1056	15	17(Q42) 13(Q52) 9(Q53)	R: C−O str (5), C−C(O)str, CO(P) str
1009	7	16(Q53) 10(Q57) 10(Q55)	1012	2	13(Q53) 10(A-52−59)8(Q42)	1016	2	18(Q53) 6(A-42−52)	P: C−O(P)str
989	4	29(Q19) 12(Q26)	993	12	21(Q19) 16(Q26)9(Q55)				Y: C−N str. P: C−O(H)str
985	20	32(Q43) 10(Q26) 8(Q39)	982	8	29(Q43) 9(Q39) 8(Q26)	992	34	29(Q43) 13(Q39) 11(Q57) 7(Q55)	R: C−O str
982	14	29(Q57) 18 (Q55) 15(A-56−60)	881	8	33(Q57) 32(Q55) 14(Q56)	982	13	47(Q57) 13(Q55) 9(Q43)	Pho: PO str (HB)[d]
971	7	15(Q26) 10(X-Q37)	973	2	11(Q26) 10(X-Q37)				P: CH oop bend, C−O str
934	15	18(Q53) 11(Q44)	936	5	13(Q53) 10(Q44)	916	7	27(Q53) 10(Q40)	R, Pho: (H2) C−O(P) str
911	3	13(Q39)	914	0.2	17(Q39)	940	15	18(Q39)	R: (N)C−C str
851	3	13(Q40) 12(Q44)	844	2	20(X-Q14) 12(Q44)10(Q40)	857	6	15(Q44) 15(Q40)	R: C−C str, C−O str
782	17	53(Q56) 9(Q20)	1052	12	18(Q56) 17(Q44) 13(Q52) 11(Q53)	766	25	84(Q56) 6(Q54)	Pho: PO str

[a] All the modes were calculated using the BVP86/TZVP level of theory with the COSMO solvent model. [b] Bond designations: Q, bonds formed by skeleton atoms (C, N, O, P); q, X−H bonds (X = C, N, O, P). Angle designations: A-Qi−Qj, A-Qi−qk, or A−qk−ql, where Qi, Oj, qk, and ql are the corresponding bonds. Hydrogen bonds: QQ hydrogen bonds O31···H41 (QQ61) and O33···H54 (QQ62). The sets of nonplanar internal coordinates include out-of-plane bendings for (i, j, k, l) atoms which are designated as X-Qi (where Qi is the out-of-plane bending bond) and torsional coordinates T-Qj, where Qj is a bond of torsion. The coordinate numbering is depicted in Figure 3. Only major contributions are shown. (See the Supporting Information for more details.) [c] Key: str, stretching; bend, bending; sym, symmetrical; asym, asymmetrical; def, deformation; rk, rocking; sc, scissoring; wa, wagging; tw, twisting; rot, rotation; oop, out-of-plane; ip, in-plane; G, guanine or 7-deazaguanine; Y, ylaminomethyl chain; P, 4,5-*cis*-dihydroxy-1-cyclopentene; R, ribose; Pho, phosphate. [d] Atom involved in the hydrogen bond.

(5.0), $H_2PO_4^-$ (7.21) to compare with deprotonation of the QMP phosphate group (6.1), and diisopropylamine (11.05) to compare with deprotonation of the secondary amine N(13) (11.2).

Let us start the consideration from the protonated state Q^+, which is stable at low pH values. The most stable *syn*/*north* conformer of Q^+ has $pK_a = 5.0$ (Table 3), which corresponds to deprotonation of the N(3) site and a $Q^+ \rightarrow Q^0$ transition. Moreover, at pH < 5.0 deprotonation ($Q^+ \rightarrow Q^0$) results in stabilization of the *anti*/*north* conformation, and a *syn* to *anti* conformation transition takes place. An alternative pathway corresponding to deprotonation ($Q^+ \rightarrow Q^0{}_{N3}$) is thermodynamically unfavorable. Since Q^0 is at least 5.36 kcal/mol more stable than $Q^0{}_{N3}$, the consequent most favorable deprotonation is $Q^0 \rightarrow Q^-{}_{ZW}$. This deprotonation proceeds at pH 6.1, and the proton leaves the $-HPO_4^-$ group. Since Q^0 is more stable than Q^- at least by 1.93 kcal/mol (Q^- population ca. 3.8%), an alternative pathway corresponding to a $Q^0 \rightarrow Q^-$ transition is also thermodynamically unfavorable. Finally, the last deprotonation ($Q^-{}_{ZW} \rightarrow Q^{2-}$) of N(13) proceeds at pH 11.2. Thus, the scheme of QMP transitions under pH changes can be summarized as follows:

$$\underset{syn/north}{Q^+} \overset{\text{pH 5.0}}{\rightleftharpoons} \underset{anti/north}{Q^0} \overset{\text{pH 6.1}}{\rightleftharpoons} \underset{anti/north}{Q^-{}_{ZW}} \overset{\text{pH 11.2}}{\rightleftharpoons} \underset{\substack{anti/north,\ 71\% \\ syn/north,\ 29\%}}{Q^{2-}} \qquad \text{(S1)}$$

Therefore, under the transition from the cationic (Q^+) to neutral (Q^0) form at pH 5.0, QMP undergoes a *syn* to *anti* conformation transition and remains in the *anti* conformation at higher pH. It should also be noted that a neutral (Q^0) form in the *anti*/*north* conformation of QMP has been observed in an X-ray crystallographic study.[2] Final deportation at a pH of about 11.2 turns QMP into the dianion (Q^{2-}), and 29% of the population adopts the *syn*/*north* conformation.

Theoretical IR Spectra. It was demonstrated above that the *anti*/*north* conformations of the Q^0 and $Q^-{}_{ZW}$ forms are the most stable in the pH range 5.0−11.2, $T = 298$ K. The analysis of

the IR-active vibrational modes for these forms was carried out (visualized spectra are presented in Figure 4). The vibrational spectra of Q^0 and Q^-_{ZW} and guanosine 5′-monophospahte (GMP) in the *north*/*anti* conformation were compared. The numbering of the atoms of Q^0 and designations of the introduced stretching coordinates are shown in Figure 3. The structure of Q^-_{ZW} in comparison to Q^0 (Figure 3) is characterized by the absence of hydrogen atom H(57). The sets of planar internal coordinates (which include all bond stretchings and all bond angles) were generated by the SPECTRUM program.[36] The sets of nonplanar internal coordinates include out-of-plane bendings and torsional coordinates, and finally, the redundant systems of internal coordinates for the neutral and anionic forms of QMP include 218 coordinates for Q^0, 215 coordinates for Q^-_{ZW}, and 139 coordinates for GMP. The details of these coordinates are provided in Table 5.

The potential energy distribution (PED) for Q^0, Q^-_{ZW}, and GMP for regions 800−1300 and 2000−3500 cm^{-1} are collected in Table 5 (a full list of the vibrational modes is presented in the Supporting Information). The visualized[51] theoretical IR spectra are presented in Figure 4. The comparison of the IR theoretical spectra of Q^0, Q^-_{ZW}, and GMP demonstrates a strong difference in the spectra of Q^0 and GMP almost in all frequency regions, while the spectra of Q^0 and Q^-_{ZW} are similar in the "fingerprint" (400−1500 cm^{-1}) region but differ in the high-frequency region.

The most evident feature of the Q^-_{ZW} IR spectrum is a very large red shift of intensive q30 stretching (N(13)H) to 2367 cm^{-1} due to the rather strong intramolecular H-bond N(13)H···O(31). In Q^0 this vibration appeared at 2796 cm^{-1} and is strongly shifted in comparison with the characteristic region of the NH_2 group stretchings (3400−3500 cm^{-1}). The stretchings of another N(13)H bond (q29) of the same NH_2 group are located at 3134 and 3156 cm^{-1} for Q^0 and Q^-_{ZW}, correspondingly, and are also red-shifted from the characteristic frequency region.

In the fingerprint region the most dramatic changes are observed in the region 800−1300 cm^{-1}, where one can see the strong changes in the relative intensities of the theoretical IR bands of Q^-_{ZW} in comparison to the calculated spectrum of Q^0. The most evident is the shift of the Q56 stretching P(30)−O(32) of Q^0 (782 cm^{-1}) to 1052 cm^{-1} (see Table 5 and Figure 4). This vibration is characterized by strong mixing with Q44 stretching in Q^-_{ZW} (Table 5). Another example is a shift of the Q57 stretching P(30)−O(33) from 1142 cm^{-1} in Q^-_{ZW} to 991 cm^{-1} in Q^-_{ZW} (see Table 5 and Figure 4).

Conclusions

In the present study it was found that the most stable neutral (Q^0) and anionic (Q^-_{ZW}) QMP forms are represented by *anti*/*north* conformations which are stabilized by strong H-bonds: O−H···O (ca. 6−15 kcal/mol) between the ribose ring and phosphate group, N−H···O (ca. 15−18 kcal/mol) between the QMP side chain and phosphate group. There is also a weak C−H···O (ca. 4 kcal/mol) H-bond between 7-deazaguanine and ribose.

Analysis of the QMP conformation transitions under a change of the QMP protonation state revealed that the nucleotide exists in the zwitterionic form with the positively charged secondary amino group (−NH_2^+−) and negatively charged phosphate group in the physiologic pH range.

A significant dependence of the relative stability of QMP conformers on the pH value has been observed. It was found that at pH 5.0 deprotonation of QMP triggers a *syn* to *anti* conformation transition. Then ca. 29% of the QMP population undergoes a reverse *anti* to *syn* transition at pH 11.2 under further deprotonation.

The IR spectra have a number of peculiarities specific for the neutral (Q^0) and anionic (Q^-_{ZW}) QMP forms in comparison to canonic guanosine 5′-monophosphate. The marker bands specific for QMP have been identified. Namely, due to H-bonding in the QMP side chain the unique vibration modes assigned to QMP NH stretchings shift to 2796 cm^{-1} in the neutral form and to 2367 cm^{-1} in the anionic form. The fingerprint region in the range of 800−1300 cm^{-1} shows dramatic changes in the stretching vibrations of the phosphate groups, ribose ring, and nucleotide side chain specific for the neutral and anionic forms in comparison to the canonic nucleotide. We believe that such shifts can be used for QMP identification.

As was pointed out by Sonavane[15] and confirmed in the current study, the side chain of QMP provides additional H-bonds: N(13)−H···O(10) and N(13)−H···O(31). The H-bond N(13)−H···O(10) has also been reported by Morris.[16] The study of the modified nucleotide confirms the assumption that the modified fragment provides additional intermolecular hydrogen bonds which could contribute to stabilization of RNA and govern enzymatic interactions. A change of the environmental pH alters the QMP conformations and might play a prominent role in biochemical functioning of QMP. Thus, we think that further investigation is needed to elucidate a role of intramolecular hydrogen bonding in biochemical interactions of QMP.

Acknowledgment. Support has been provided by NSF CREST Grant HRD-0833178. We are grateful to the Mississippi Center for Supercomputer Research for the computational facilities. D.K. thanks Roman I. Zubatyuk for his invaluable help with fine-tuning of the Jackson State University high-performance computing systems. This work was partly supported by the exchange program of Jackson State University. G.M.K. also thanks the RFBR (Grant No. 08-03-00415a) for partial financial support.

Supporting Information Available: Full list of IR modes of neutral (Q^0) and anionic (Q^{-1}_{ZW}) forms of QMP in the *north*/*anti* conformation compared with canonic GMP. This material is available free of charge via the Internet at http://pubs.acs.org.

References and Notes

(1) Kasai, H.; Kuchino, Y.; Nihei, K.; Nishimura, S. *Nucleic Acids Res.* **1975**, *2*, 1931.
(2) Yokoyama, S.; Miyazawa, T.; Iitaka, Y.; Yamaizumi, Z.; Kasai, H.; Nishimura, S. *Nature* **1979**, *282*, 107.
(3) Morris, R. C.; Elliott, M. S. *Mol. Genet. Metab.* **2001**, *74*, 147.
(4) Gündüz, U.; Elliott, M. S.; Seubert, P. H.; Houghton, J. A.; Houghton, P. J.; Trewyn, R. W.; Katze, J. R. *Biochim. Biophys. Acta* **1992**, *1139*, 229.
(5) Baranowski, W.; Dirheimer, G.; Jakowicki, J. A.; Keith, G. *Cancer Res.* **1994**, *54*, 4468.
(6) Aytac, U.; Gündüz, U. *Cancer Biochem. Biophys.* **1996**, *14*, 93.
(7) Huang, B.-S.; Wu, R.-T.; Chien, K.-Y. *Cancer Res.* **1992**, *52*, 4696.
(8) Emmerich, B.; Zubrod, E.; Weber, H.; Maubach, P. A.; Kersten, H.; Kersten, W. *Cancer Res.* **1985**, *45*, 4308.
(9) Dovbeshko, G. I.; Gridina, N. Y.; Kruglova, E. B.; Pashchuk, O. P. *Talanta* **2000**, *53* (1), 233.
(10) Dovbeshko, G. I.; Chegel, V. I.; Gridina, N. Y.; Repnytska, O. P.; Shirshov, Y. M.; Tryndiak, V. P.; Todor, I. M.; Solyanik, G. I. *Biopolymers* **2002**, *67* (6), 470.
(11) Iwata-Reuyl, D. *Curr. Opin. Chem. Biol.* **2008**, *12*, 126.
(12) Lee, B. W. K.; Van Lanen, S. G.; Iwata-Reuyl, D. *Biochemistry* **2007**, *46* (44), 12844.
(13) Cicmil, N.; Shi, L. *Acta Crystallogr., F* **2008**, *64* (2), 119.
(14) Tidten, N.; Stengl, B.; Heine, A.; Garcia, G. A.; Klebe, G.; Reuter, K. *J. Mol. Biol.* **2007**, *374* (3), 764.

(15) Sonavane, U. B.; Sonawane, K. D.; Tewari, R. *J. Biomol. Struct. Dyn.* **2002**, *20* (3), 473.
(16) Morris, R. C.; Brown, K. G.; Elliott, M. S. *J. Biomol. Struct. Dyn.* **1999**, *16* (4), 757.
(17) Gorb, L.; Shishkin, O.; Leszczynski, J. *J. Biomol. Struct. Dyn.* **2005**, *22* (4), 441.
(18) Kosenkov, D.; Gorb, L.; Shishkin, O. V.; Šponer, J.; Leszczynski, J. *J. Phys. Chem. B* **2008**, *112* (1), 150.
(19) Shishkin, O. V.; Gorb, L.; Zhikol, O. A.; Leszczynski, J. *J. Biomol. Struct. Dyn.* **2004**, *22* (2), 227.
(20) Shishkin, O. V. *Chem. Phys. Lett.* **2008**, *458* (1−3), 96.
(21) Jang, Y. H.; Goddard, W. A., III; Noyes, K. T.; Sowers, L. C.; Hwang, S.; Chung, D. S. *J. Phys. Chem. B* **2003**, *107* (1), 344.
(22) You, T. J.; Bashford, D. *Biophys. J.* **1995**, *69* (5), 1721.
(23) Makarov, V.; Pettitt, B. M.; Feig, M. *Acc. Chem. Res.* **2002**, *35* (6), 376.
(24) Klamt, A.; Schüürmann, G. *J. Chem. Soc., Perkin Trans. 2* **1993**, 799.
(25) Klamt, A.; Eckert, F.; Hornig, M.; Beck, M. E.; Bürger, T. *J. Comput. Chem.* **2002**, *23*, 275.
(26) Klamt, A. *Fluid Phase Equilib.* **2003**, *206*, 223.
(27) Eckert, F.; Klamt, A. *AIChE J.* **2002**, *48*, 369.
(28) Eckert, F.; Klamt, A. *COSMOtherm*, version C.2.1, release 01.05; COSMOlogic GmbH & Co. KG: Leverkusen, Germany, 2005.
(29) Murugan, N. A.; Hugosson, H. W. *J. Phys. Chem. B* **2009**, *113*, 1012.
(30) Saenger, W. In *Principles of Nucleic Acid Structure*; Cantor, C. R., Ed.; Springer-Verlag: New York, 1984.
(31) Frisch, M. J.; Trucks, G. W.; Schlegel, H. B.; Scuseria, G. E.; Robb, M. A.; Cheeseman, J. R.; Montgomery, J. A., Jr.; Vreven, T.; Kudin, K. N.; Burant, J. C.; Millam, J. M.; Iyengar, S. S.; Tomasi, J.; Barone, V.; Mennucci, B.; Cossi, M.; Scalmani, G.; Rega, N.; Petersson, G. A.; Nakatsuji, H.; Hada, M.; Ehara, M.; Toyota, K.; Fukuda, R.; Hasegawa, J.; Ishida, M.; Nakajima, T.; Honda, Y.; Kitao, O.; Nakai, H.; Klene, M.; Li, X.; Knox, J. E.; Hratchian, H. P.; Cross, J. B.; Bakken, V.; Adamo, C.; Jaramillo, J.; Gomperts, R.; Stratmann, R. E.; Yazyev, O.; Austin, A. J.; Cammi, R.; Pomelli, C.; Ochterski, J. W.; Ayala, P. Y.; Morokuma, K.; Voth, G. A.; Salvador, P.; Dannenberg, J. J.; Zakrzewski, V. G.; Dapprich, S.; Daniels, A. D.; Strain, M. C.; Farkas, O.; Malick, D. K.; Rabuck, A. D.; Raghavachari, K.; Foresman, J. B.; Ortiz, J. V.; Cui, Q.; Baboul, A. G.; Clifford, S.; Cioslowski, J.; Stefanov, B. B.; Liu, G.; Liashenko, A.; Piskorz, P.; Komaromi, I.; Martin, R. L.; Fox, D. J.; Keith, T.; Al-Laham, M. A.; Peng, C. Y.; Nanayakkara, A.; Challacombe, M.; Gill, P. M. W.; Johnson, B.; Chen, W.; Wong, M. W.; Gonzalez, C.; Pople, J. A. *Gaussian 03*, revision C.02; Gaussian, Inc.: Wallingford, CT, 2004.
(32) Becke, A. D. *Phys. Rev. A* **1988**, *38*, 3098.
(33) Becke, A. D. *J. Chem. Phys.* **1993**, *98*, 5648.
(34) Schaefer, A.; Horn, H.; Ahlrichs, R. *J. Chem. Phys.* **1992**, *97*, 2571.
(35) Schaefer, A.; Huber, C.; Ahlrichs, R. *J. Chem. Phys.* **1994**, *100*, 5829.
(36) Yagola, A. G.; Kochikov, I. V.; Kuramshina, G. M.; Pentin, Yu. A. *Inverse Problems of Vibrational Spectroscopy*; VSP: Zeist, The Netherlands, 1999.
(37) Kuramshina, G. M.; Weinhold, F. A.; Kochikov, I. V.; Pentin, Yu. A.; Yagola, A. G. *J. Chem. Phys.* **1994**, *100* (2), 1414.
(38) Kerestury, G.; Jalkovsky, G. *J. Mol. Struct.* **1971**, *10*, 304.
(39) Cyvin, S. J.; Brunvoll, J. *J. Mol. Spectrosc.* **1971**, *40*, 431.
(40) Bader, R. W. F. *Atoms in Molecules: A Quantum Theory*; Oxford University Press: Oxford, U.K., 1990.
(41) Biegler-König, F.; Schönbohm, J.; Bayles, D. *J. Comput. Chem.* **2001**, *22*, 545.
(42) Shishkin, O. V.; Palamarchuk, G. V.; Gorb, L.; Leszczynski, J. *J. Phys. Chem. B* **2006**, *110*, 4413.
(43) Koch, U.; Popelier, P. *J. Phys. Chem.* **1995**, *99*, 9747.
(44) Popelier, P. L. A. *J. Phys. Chem. A* **1998**, *102*, 1873.
(45) Bader, R. F. W.; Slee, T. S.; Cremer, D.; Kraka, E. *J. Am. Chem. Soc.* **1983**, *105*, 5061.
(46) Kosenkov, D.; Gorb, L.; Shishkin, O. V.; Šponer, J.; Leszczynski, J. *J. Phys. Chem. B* **2008**, *112* (1), 150.
(47) Lyssenko, K. A.; Antipin, M. Yu. *Russ. Chem. Bull.* **2006**, *55* (1), 1.
(48) Espinosa, E.; Molinsa, E.; Lecomte, C. *Chem. Phys. Lett.* **1998**, *285* (3−4), 170.
(49) Lyssenko, K. A.; Korlyukov, A. A.; Golovanov, D. G.; Ketkov, S. Yu.; Antipin, M. Yu. *J. Phys. Chem. A* **2006**, *110* (20), 6545.
(50) March, J. *Advanced Organic Chemistry*, 3rd ed.; John Wiley: New York, 1985.
(51) ChemCraft (version 1.5), http://www.chemcraftprog.com.

JP903993S